Mathematical Modeling and Dynamic Simulation of a Class of Drive Systems with Permanent Magnet Synchronous Motors

M. Mikhov[a,*]

[a]*Faculty of Automatics, Technical University of Sofia, 8 Kliment Ohridski Blvd., 1757 Sofia, Bulgaria*

Abstract

The performance of a two-coordinate drive system with permanent magnet synchronous motors is analyzed and discussed in this paper. Both motors have been controlled in brushless DC motor mode in accordance with the rotor positions. Detailed study has been carried out by means of mathematical modeling and computer simulation for the respective transient and steady-state regimes at various load and work conditions. The research carried out as well as the results obtained can be used in the design, optimization and tuning of such types of drive systems. They could be also applied in the teaching process.

1. Introduction

A number of applications in the mechanical industry require two-coordinate drive systems with good static, dynamic and energetic characteristics. In recent years, permanent magnet synchronous motors (PMSM) have been used in such cases, because they have some advantages, including: compact form; low power loss and high efficiency; high power/mass ratio; good heat dissipation characteristics; low rotor inertia and good dynamics; high speed capabilities.

Applying some control methods, drive systems with such motors can combine the advantages of both DC and AC motor systems. For example, the PMSM electric drives performance improves significantly if their control is executed according to the rotor position. Thus commutation flexibility is provided, avoiding the risk of synchronization failure in case of overload [1, 2, 7, 8].

The complexity of electromechanical systems makes them difficult for description and study in some cases. For this reason, mathematical modeling and computer simulation are widely applied for the purpose of their analysis and synthesis. Such an approach provides for very good conditions to investigate electric drives behavior in various transient and steady-state working regimes, which is not always convenient or possible in industrial and laboratory environments [3, 4, 5, 6].

This paper considers a two-coordinate electromechanical system with permanent magnet synchronous motors, which are controlled in brushless DC motor mode. Detailed study has been carried out by means of modeling and computer simulation for the respective dynamic and static regimes at different operation modes. Behavior analysis has been made aiming at improvement of the drive system performance.

---

*Corresponding author. Tel.: +359 2 965 29 46, e-mail: mikhov@tu-sofia.bg.

2. Mathematical modeling of the drive system

2.1. Features of the drive system

A simplified block diagram of the drive system under consideration is represented in fig. 1, where the notations are as follows: PC – position controller; SC1, SC2 – speed controllers; RC1, RC2 – current reference blocks; CC1, CC2 – three-phase current controllers; IC1, IC2 – inverter control blocks; VI1, VI2 – voltage source inverters; UR – uncontrollable rectifier; C – filter capacitor; PS1, PS2 – position sensors; PF1, PF2 – position feedback blocks; SF1, SF2 – speed feedback blocks; M1, M2 – motors; L1, L2 – loads at the respective coordinate axes; V_{sr_1}, V_{sr_2} – speed reference signals; V_{cr_1}, V_{cr_2} – current reference signals; V_{pf_1}, V_{pf_2} – position feedback signals; V_{sf_1}, V_{sf_2} – speed feedback signals; V_{cf_1}, V_{cf_2} – current feedback signals; V_d – DC link voltage; ω_1, ω_2 – motor speeds; θ_1, θ_2 – angular positions; T_{l_1}, T_{l_2} – load torques applied to the respective motor shafts.
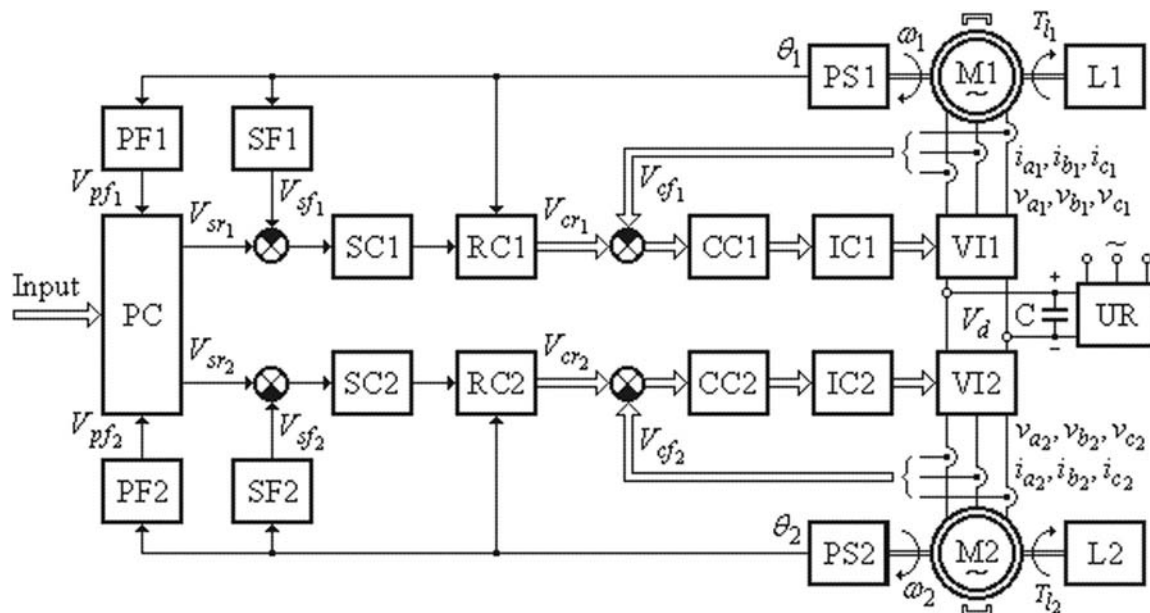

Fig. 1. Block diagram of the drive system under consideration

The motors used are characterized by having permanent magnet-produced fields on the rotors and armature windings on the stators. Both subsystems have identical cascade structures with subordinate regulation. The motors have been controlled in brushless DC motor mode in accordance with the respective rotor positions. Control loops optimization and tuning have been done sequentially, starting from the innermost ones.

2.2. Mathematical description

In order to obtain a suitable simulation model some assumptions have been made, such as:

- motors are unsaturated;
- eddy-currents and hysteresis effects have negligible influence on the stator currents;
- motors are symmetrical three-phase machines;
- self and mutual inductances are constant and independent of the rotor position;
- devices in the power-electronic circuits are ideal.

Fig. 2 shows the equivalent circuit diagram of PMSM and the voltage source inverter for one coordinate axis. The corresponding notations are as follows: S1÷S6 – power electronic switches; D1÷D6 – freewheeling diodes; v_a, v_b, v_c – voltages applied on stator phases a, b and c respectively; i_a, i_b, i_c – phase currents; e_a, e_b, e_c – back EMF voltages; R_a, R_b, R_c – stator phase resistances; L_a, L_b, L_c – phase self inductances; L_{ba}, L_{ca}, L_{cb} – mutual inductances.
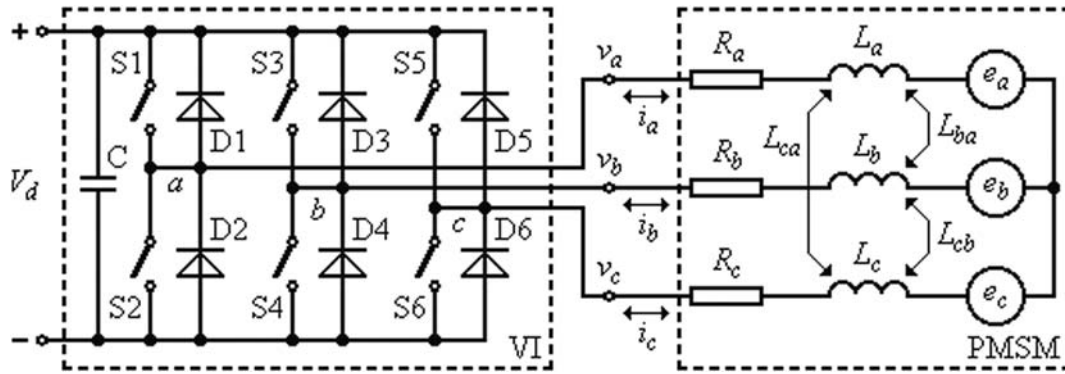

Fig. 2. Equivalent circuit diagram of PMSM and the voltage source inverter

The vector-matrix model of such a set is described as follows:

$$
\begin{bmatrix} v_a \\ v_b \\ v_c \end{bmatrix} = \begin{bmatrix} R_s & 0 & 0 \\ 0 & R_s & 0 \\ 0 & 0 & R_s \end{bmatrix} \begin{bmatrix} i_a \\ i_b \\ i_c \end{bmatrix} + \begin{bmatrix} L_a & L_{ba} & L_{ca} \\ L_{ba} & L_b & L_{cb} \\ L_{ca} & L_{cb} & L_c \end{bmatrix} \frac{\mathrm{d}}{\mathrm{d}t} \begin{bmatrix} i_a \\ i_b \\ i_c \end{bmatrix} + \begin{bmatrix} e_a \\ e_b \\ e_c \end{bmatrix} , \quad (1)
$$

where $R_s = R_a = R_b = R_c$ is the stator phase resistance.

The back EMF voltage waveforms are expressed by the equation:

$$
\begin{bmatrix} e_a \\ e_b \\ e_c \end{bmatrix} = \omega \frac{\mathrm{d}}{\mathrm{d}\theta} \begin{bmatrix} \Phi_a \\ \Phi_b \\ \Phi_c \end{bmatrix} , \quad (2)
$$

where Φ_a, Φ_b, Φ_c are the stator magnetic fluxes of the motor phases a, b and c respectively.

Since the motor windings are star connected (fig. 2), the next relation is valid:

$$
i_a + i_b + i_c = 0. \quad (3)
$$

Assuming there is no change in the rotor reluctance with angular position, then:

$$
\begin{aligned}
L_a &= L_b = L_c = L; \quad &(4) \\
L_{ba} &= L_{ca} = L_{cb} = M. \quad &(5)
\end{aligned}
$$

Taking into consideration Eqs. (4) and (5), the vector-matrix Eq. (1) is arranged as follows:

$$
\begin{bmatrix} v_a \\ v_b \\ v_c \end{bmatrix} = R_s \begin{bmatrix} i_a \\ i_b \\ i_c \end{bmatrix} + L_s \frac{\mathrm{d}}{\mathrm{d}t} \begin{bmatrix} i_a \\ i_b \\ i_c \end{bmatrix} + \begin{bmatrix} e_a \\ e_b \\ e_c \end{bmatrix} , \quad (6)
$$

where $L_s = L - M$ is the stator phase inductance.

The motor electromagnetic torque can be expressed as:

$$T = \frac{e_a i_a + e_b i_b + e_c i_c}{\omega},\tag{7}$$

and the mechanical dynamics equations are as follows:

$$J\frac{\mathrm{d}\omega}{\mathrm{d}t} = T - T_l - D\omega;\tag{8}$$

$$\frac{\mathrm{d}\theta}{\mathrm{d}t} = \omega,\tag{9}$$

where J is the total inertia referred to the respective motor shaft; D – the viscous damping coefficient.

3. Computer simulation and performance analysis

Every specific working regime of the two-coordinate drive system requires an appropriate control algorithm. For this reason, using the MATLAB/SIMULINK software package some computer simulation models have been developed to analyze the system under consideration.

Detailed investigation has been carried out by means of mathematical modeling and computer simulation for the respective transient and steady-state regimes at various working conditions.

3.1. Phase currents formation

The current controllers have a programmable hysteresis band which determines the respective modulation frequency.

Fig. 3 illustrates the principle of current pulses formation. The used notations are as follows: i_r – reference phase current waveform; $2\Delta i_r = i_{\max} - i_{\min}$ – reference hysteresis band; $i_{\max}$ and $i_{\min}$ – maximum and minimum current values, respectively; $T_m = t_{on} + t_{off}$ – modulation period.
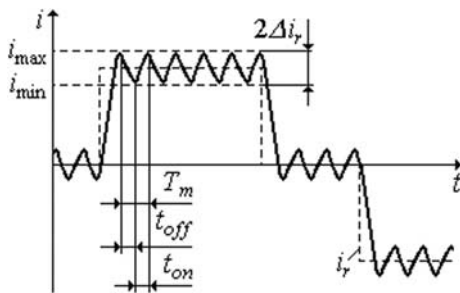

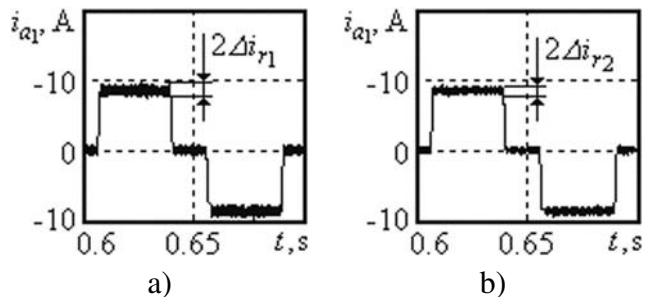Fig. 3. Principle of current pulses formation

Fig. 4. Influence of the hysteresis band

The modulation frequency is expressed by:

$$f_m = \frac{1}{T_m}.\tag{10}$$

The hysteresis band influence of the first current controller is shown in fig. 4. It represents the phase current waveforms for two different hysteresis bands ($2\Delta i_{r_1}$ and $2\Delta i_{r_2}$ respectively). As evident, narrowing the zone, i.e. increasing the chopping frequency will result in reduction of the current pulsations.

The analysis carried out shows that this frequency is not of a constant value and depends on the following factors:

– hysteresis band;

– reference motor speed;

– power circuit electromagnetic time-constant;

– initial current value.

This analysis allows selecting of the optimal hysteresis band in accordance with the respective power switches. In the research carried out the maximum modulation frequency has been limited to a value of $f_{m\,max} < 8\,000$ Hz.

Fig. 5 illustrates the dynamic maintenance of zero phase current in the respective interval by means of pulse width modulation.
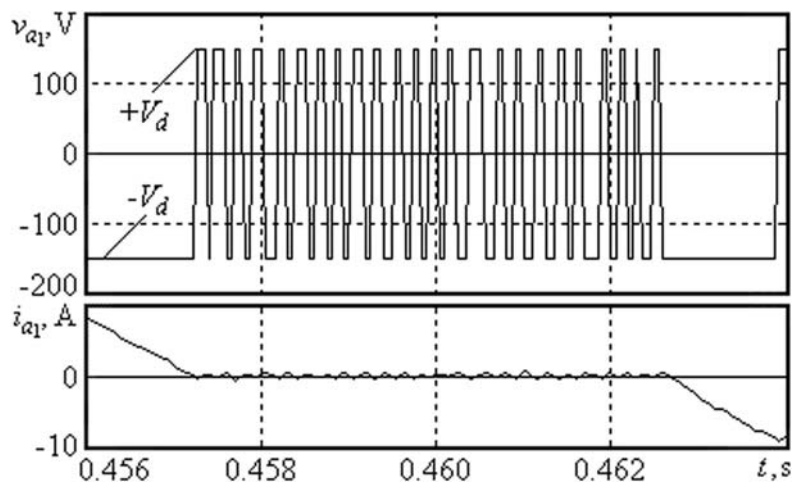
Fig. 5. Dynamic maintenance of zero phase current

Fig. 6 shows the phase current waveform i_{a_1} and the respective trapezoidal back EMF voltage e_{a_1}. In this case the simulation results have been obtained for a quasi-steady-state regime at rated load applied to the motor shaft.

The three-phase current waveforms i_{a_1}, i_{b_1}, and i_{c_1} for the same load torque are represented in fig. 7.
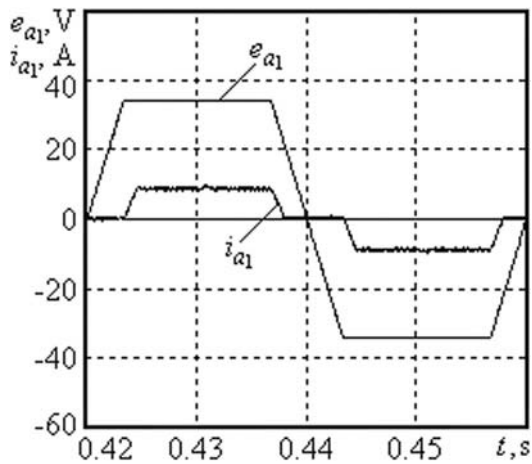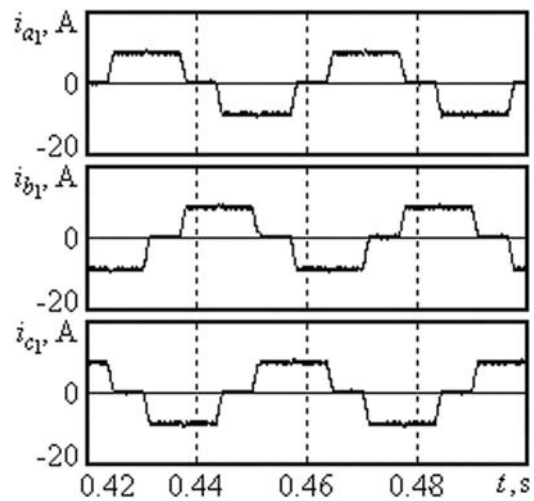
Fig. 6. Phase current and back EMF voltage

Fig. 7. Three-phase current waveforms

3.2. Breaking regime

Various breaking modes have been investigated aiming at fast and efficient stopping and reversing. Some time-diagrams obtained at reverse speed control with electrical braking are shown in fig. 8, where T_{b1} is the braking torque. The reference speed values in this case are $\pm\omega_{1r} = \pm157$ rad/s. As evident, the braking mode applied ensures good dynamics with maximum reverse time less than 0.1 s.

3.3. Current limitation and speed stabilization

The phase currents limitation is provided through the current reference signals, formed by the respective speed controllers. These controllers have been optimized in such a way, that the static errors possibly caused by disturbances are eliminated.

Fig. 9 illustrates motor speed stabilization when the load torque changes. The respective transient and steady-state regimes are represented, as well as the drive system reaction to a disturbance expressed as load change.
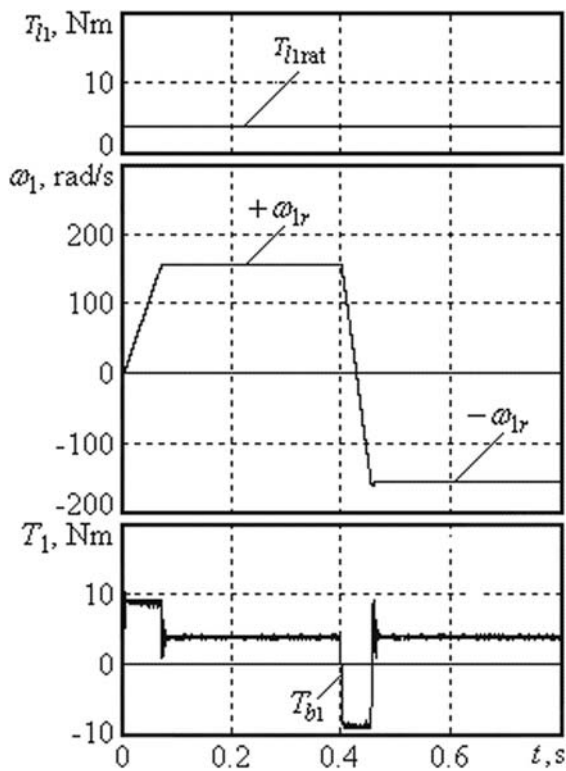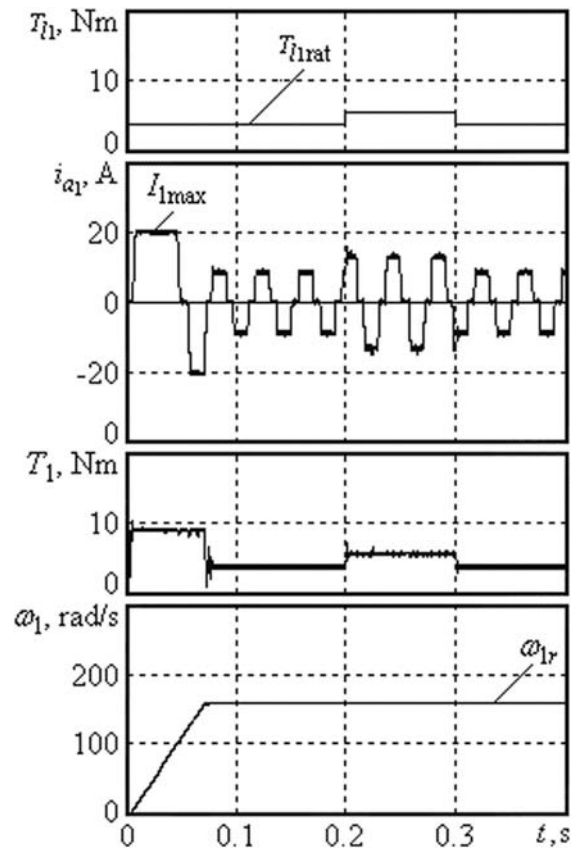
Fig. 8. Reversing with electrical breaking   Fig. 9. Current limitation and speed stabilization

In this case the load torque applied is equal to the rated value $T_{l1\mathrm{rat}}$ and the respective disturbance is $\Delta T_{l_1} = 0.5 T_{l_1\mathrm{rat}}$. The load change is applied during the time interval of $t = (0.2\,\mathrm{s} \div 0.3\,\mathrm{s})$. As evident, at an appropriate tuning of the speed controller, static speed error does not appear when T_{l_1} changes. The reference speed is $\omega_{1r} = 157$ rad/s and the starting current is limited to the maximum admissible value of $I_{1\max}$, which provides for a maximum starting motor torque.

3.4. Two-coordinate position control

Two algorithms for trajectory formation have been investigated, namely simultaneous and consecutive movements along both coordinate axes.

Fig. 10 represents some simulation results obtained for two-coordinate position control with consecutive motion along the coordinate axes. The reference distances are indicated with θ_{1r} and θ_{2r} respectively.
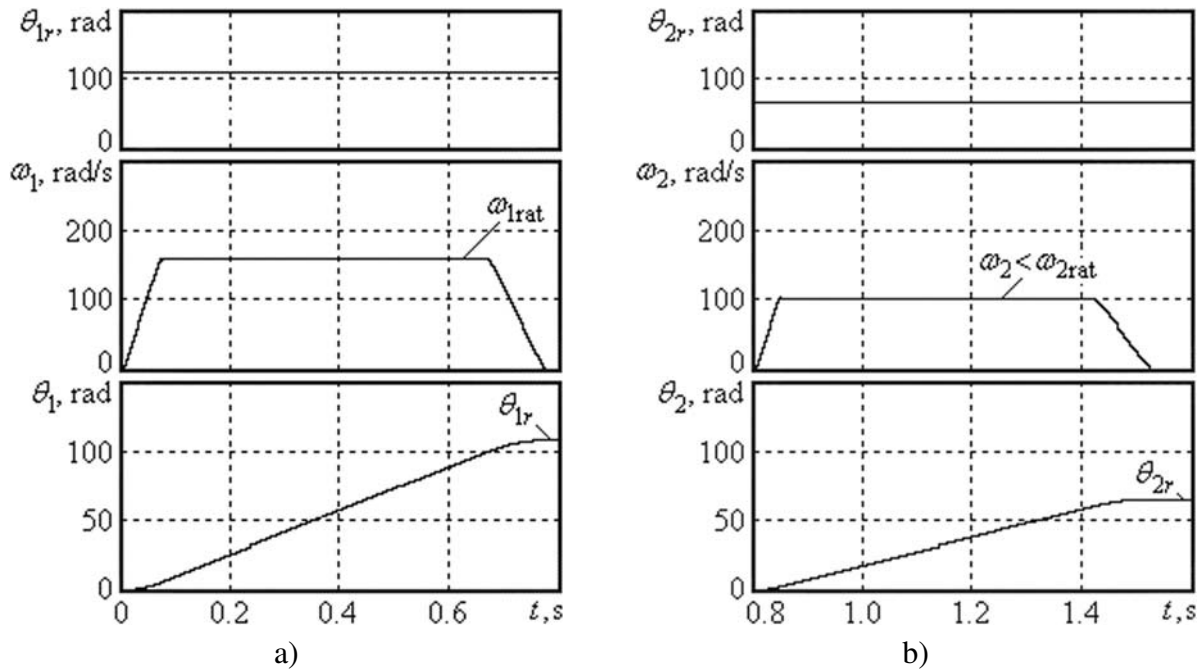

Fig. 10. Time-diagrams for consecutive position control along both coordinate axes

Fig. 10a illustrates the realization of a reference motion along the first coordinate axis. The respective motor works at maximum speed of $\omega_1 = \omega_{1\mathrm{rat}}$, which ensures fast operation of the drive system.

Fig. 10b shows the subsequent positioning along the second coordinate axis. In this case the movement is carried out with a lower speed of $\omega_2 < \omega_{2\mathrm{rat}}$.
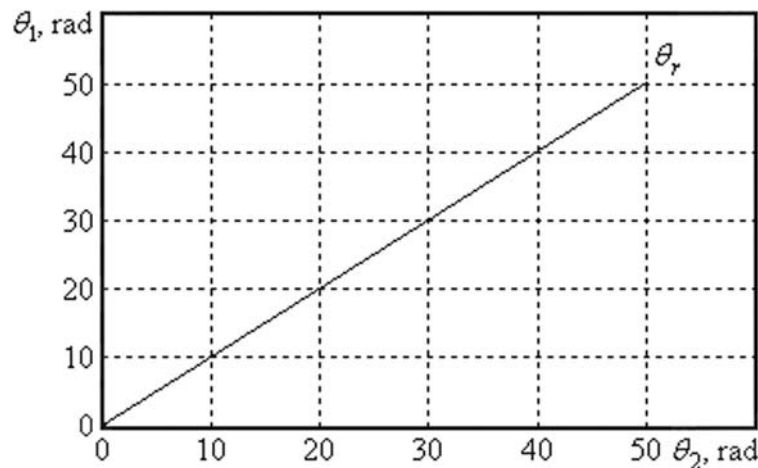

Fig. 11. Trajectory of simultaneous movement along both coordinate axes

A simultaneous movement along both coordinate axes is illustrated in fig. 11, when the two motor speeds are equal.

The motors used are identical, both with rated power $P_{\mathrm{rat}} = 0.6\,\mathrm{kW}$ and rated angular speed $\omega_{\mathrm{rat}} = 157\,\mathrm{rad/s}$.

4. Conclusion

The performance of a two-coordinate drive system with permanent magnet synchronous motors has been discussed in this paper. Both motors have been controlled in brushless DC motor mode in accordance with the respective rotor positions.

Using the MATLAB/SIMULINK software package a number of computer simulation models have been developed to analyze this class of drive systems. Detailed study has been carried out for the dynamic and static regimes at various loads, disturbances and work conditions.

The analysis shows that the control approach applied ensures good performance, which makes it suitable for a variety of applications in the mechanical industry.

The research carried out as well as the results obtained can be used in the design, optimization and tuning of such types of drive systems. They could be also applied in the teaching process.

Acknowledgements

References

[1] Boldea, I., Nasar, S. A., Electric drives, CRC, Boca Raton, 1999.
[2] Chen, C., Cheng, M., A new cost effective sensorless commutation method for brushless DC motors without phase shift circuit and neutral voltage, IEEE Trans. on Power Electronics, 2 (22) (2007) 644–653.
[3] Mikhov, M. R., Investigation of a permanent magnet synchronous motor control system, Technical Ideas, 3/4 (38) (2001) 23–34.
[4] Mikhov, M. R., Analysis and simulation of a servo drive system with hysteresis current control, Proceedings of the International Conference on Automatics and Informatics, Sofia, Bulgaria, 2002, pp. 197–200.
[5] Ong, C., Dynamic simulation of electric machinery using MATLAB/SIMULINK, Prentice Hall, New Jersey, 1998.
[6] Safi, S. K., Acarnley, P. P., Jack, A. G., Analysis and simulation of the high-speed torque performance of brushless DC motor drives, IEE Proceedings – Electric Power Applications, 3 (142) (1995) 191–200.
[7] Sozer, Y., Torrey, D. A., Adaptive torque ripple control of permanent magnet brushless DC motors, Proceedings on the Applied Power Electronics Conference, Anaheim, USA, 1998, pp. 86–92.
[8] Yoon, Y., Kim, D., Lee, T., Choe, Y., Won, C., A low cost speed control system of PM brushless DC motor using 2 Hall-Ics, Proceedings of the International Conference on Mechatronics and Information Technology, Jecheon, Korea, 2003, pp. 150–155.